Structural Monitoring and Maintenance, *Vol. 5, No. 1 (2018) 39-50*
DOI: https:// doi.org/10.12989/smm.2018.5.1.039

The compression-shear properties of small-size seismic isolation rubber bearings for bridges

Yi-feng Wu[1,2], Hao Wang[*2], Ben Sha[2], Rui-jun Zhang[2] and Ai-qun Li[3]

[1]*School of Civil and Transportation Engineering, Beijing University of Civil Engineering and Architecture, Beijing, 100044, China*
[2]*School of Civil Engineering, Southeast University, Nanjing, 210096, China*
[3]*Beijing Advanced Innovation Center for Future Urban Design, Beijing University of Civil Engineering and Architecture, Beijing, 100044, China*

(Received November 15, 2017, Revised February 2, 2018, Accepted February 14, 2018)

Abstract. Taking three types of bridge bearings with diameter being 100 mm as examples, the theoretical analysis, the experimental research as well as the numerical simulation of these bearings is conducted. Since the normal compression and shear machines cannot be applied to the small-size bearings, an improved equipment to test the properties of these bearings is proposed and fabricated. Besides, the simulation of the bearings is conducted based on the explicit finite element software ANSYS/LS-DYNA, and some parameters of the bearings are modified in the finite element model to reduce the computation cost effectively. Results show that all the research methods are capable of revealing the fundamental properties of the small-size bearings, and a combined use of these methods can better catch both the integral properties and the inner detailed mechanical behaviors of the bearings.

Keywords: small-size; compression-shear; ANSYS/LS-DYNA; explicit algorithm; contact analysis

1. Introduction

For decades, there have been many earthquakes around the world, and their destructive power is alarming. In order to improve the seismic performance of the engineering structure, researchers put forward a variety of seismic technologies, such as passive control, active control and intelligent control. The passive control technology mainly separates the structure from the ground through the isolation equipments to reduce the seismic force and seismic energy transmitted to the superstructure. At present, the seismic isolation equipments that have been successfully used in bridge engineering are mainly plate rubber bearings, lead rubber bearings, high damping rubber bearings and friction pendulum bearings.

In recent years, the theoretical, experimental and numerical simulations of the mechanical properties of isolation equipments have received much attention of researchers. Kelly *et al*. (1978) put forward the theory and design method of laminated rubber bearings. Tyler and Robinson (1984) conducted a large deformation loading test on lead rubber bearings and concluded that the horizontal shear performance of lead rubber bearings can be simplified to be bilinear. Hwang *et al*.

*Corresponding author, Professor, E-mail: wanghao1980@seu.edu.cn

http://www.techno-press.org/?journal=smm&subpage=7 ISSN: 2288-6605 (Print), 2288-6613 (Online)

(1996) proposed the equivalent linearization model of the bearings. Constantinou *et al*. (1987) proposed the formula of friction coefficient between steel and teflon surface by experiments. Abe *et al*. (2004) investigated the hysteretic behaviors of three types of laminated rubber bearings under multi-axial loading. Warn *et al*. (2007) studied the influence of lateral deformation of the rubber bearings on its vertical stiffness. Han *et al*. (2014) investigated the stability characteristics of the isolated bearings and put forward the corresponding theoretical model. In China, Liu and Zhou (1999) systematically studied the basic mechanical properties, various correlations and long-term performances of natural rubber bearings and lead rubber bearings. In the research of numerical simulation of isolated bearings, Takayama *et al*. (1994) conducted a large deformation nonlinear finite element analysis of laminated rubber bearings, in which the rubber material model parameters were obtained by biaxial tensile tests. Ali and Abdel-Ghaffar (1995) carried out the fine finite element numerical simulation of the lead rubber bearings and applied the simplified mechanics model of the lead rubber bearings to the isolation design of the cable-stayed bridge. Yoshida *et al*. (2004) presented a novel constitutive model to describe the mechanical behavior of high-damping rubber bearings. Wang *et al*. (2014) simulated the laminated rubber bearings using LS-DYNA software based on experimental data. Wu *et al*. (2017) conducted a numerical simulation of a sliding lead rubber bearings based on explicit finite element method and conducted test verifications.

Generally, experimental studies on the mechanical properties of common rubber bearings are becoming more and more sophisticated. However, the modeling of the contact between different parts and the large deformation of rubber still needs to be further studied in the numerical simulation of bearings. In addition, the size of the bearings in the above study is similar to that in actual projects, most of the bearings' diameter is in the range between 300 mm and 1100 mm. With the further popularization and application, bearings with diameter less than 200 mm also gradually emerge in small span bridges (SAC 2007). In addition, the smaller size rubber bearings (Zhang *et al.* 2001, Wei *et al.* 2018) may be used in the shake table tests of the scaled isolated bridges, while there are few systematic studies on the mechanical properties of such small-size bearings.

In this study, the basic mechanical properties of three types of small size rubber bearings are explored through theoretical analysis, experimental research and numerical simulations. The three types of bearings are sliding lead rubber bearing, sliding rubber bearing and lead rubber bearing respectively. And the calculated results obtained by different methods are compared with each other.

2. Isolation bearings

The diameter of all the small bearings described in this article is 100 mm, the detailed design parameters of the bearings are listed in Table 1. The overall and partial details of each bearing are shown in Fig. 1. The sliding lead rubber bearing is a combination of the teflon plate sliding bearing and the lead rubber bearing. The gap between the baffle and the upper cover in the sliding lead rubber bearing in Fig. 1(a) is 5 mm, while the gap in the sliding plate bearing in Fig. 1(c) is 10 mm.

Table 1 Mechanical parameters of the seismic isolation bearings

Parameter	Value
Type of steel plate	Q235
Shear modulus of rubber (MPa)	0.8Mpa
Diameter of the rubber	100 mm
Diameter of the lead core (mm)	16 mm
Rubber plate (thickness × number of layers)	2.5×8=20 mm
Steel plate (thickness × number of layers)	1.6×7=11.2 mm

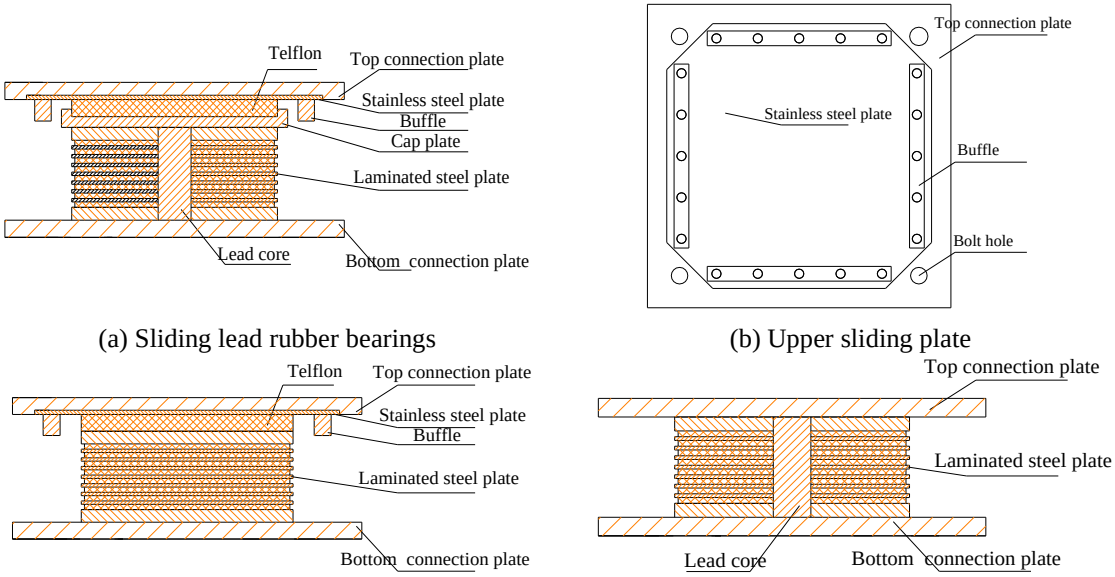

(a) Sliding lead rubber bearings (b) Upper sliding plate

(c) Sliding rubber bearings (d) Lead rubber bearing

Fig. 1 The design drawings of different bearings

3. Theoretical research

The mechanical properties of rubber bearings include vertical compression stiffness, compression-shear hysteresis performance, ultimate deformation capacity, stability and anti-fatigue aging ability (SAC 2007). This study only studies the most critical and interesting compression-shear properties of the three bearings.

3.1 Laminated rubber bearings

According to Haringx's elasticity theory of small deformation, the compression-shear horizontal stiffness, K_h, of laminated rubber bearings is calculated as follows

$$K_h = \frac{P^2}{2k_{rl}q_l \tan(\frac{q_l H}{2}) - PH} \tag{1}$$

$$q_l = \sqrt{\frac{P}{k_{rl}}(\frac{P}{k_s}+1)} \tag{2}$$

where P is the axial pressure load, H is the sum of the thickness of the laminated rubber and the laminated steel. The effective bending stiffness, $k_{rl} = (EI)_{eff} = E_{rb}IH / T_r$, the modified compression modulus of elasticity, $E_{rb} = E_r E_b / (E_r + E_b)$, E_r is the elastic modulus considering bending, and $E_r = 3G(1+2\kappa S_1^2 / 3)$. The effective shear stiffness, $k_s = (EI)_{eff} = GAH / T_r$, in which T_r is the total thickness of rubber layers, G is the shear modulus and A is the bonded area of rubber.

According to Eq. (1), the horizontal shear stiffness of the plate bearing in this study is 0.298 kN/mm under the small deformation condition when the axial pressure, P, is set as 25.5 kN, in contrast, the shear stiffness without considering vertical pressure is 0.314 kN/mm.

3.2 Lead rubber bearings

The nonlinear models of horizontal shear performances for lead rubber bearings mainly include the bilinear model given by Japan's seismic design regulations (MCJ 1994) and the modified bilinear model given by New Zealand MWD CDP818 (Mori *et al*. 1999). Taking the former as an example, the calculation formulas are presented as follows

$$F = A_R G\gamma + A_p q \tag{3}$$

$$K_2 = \frac{F - Q}{u} \tag{4}$$

$$Q = A_p q_0 \tag{5}$$

$$K_1 = 6.5K_2 \tag{6}$$

where, A_R, A_p denote the area of the rubber layer and the lead core, γ denotes the shear strain of rubber, F is the resilience of the bearing, q is the average shear stress of the lead core section, q_0 corresponds to the lead shear stress with the shear strain being zero, Q indicates the characteristic strength of the bearing, u is the displacement of the bearing, K_1 is the pre-yield stiffness and K_2 is the stiffness after yielding.

According to Eqs. (3)-(6), it can be seen that the theoretical yield strength of the lead rubber bearing described in this paper is 0.221 kN / mm with the shear deformation 100%.

4. Experimental research

4.1 Loading equipment

The diameter of the bearings studied in this article is 100 mm, while there are few suitable

compression-shear equipments to conduct the compression-shear test for such small-size bearings, the main reason is that the design vertical force of the bearing is relatively small. For example, 10 Mpa surface pressure only corresponds to 78.5 kN, a slight deviation of the vertical load from the normal compression-shear equipment may cause bearings instability, damage and other issues, and at the same time, the accuracy is difficult to control. Therefore, this article independently designed and manufactured a compression-shear equipment specifically for small-size bearings, the facade design and molding diagram of the equipment are shown in Fig. 2.

4.2 Test conditions

Considering that the shear hysteretic behavior of the bearing is closely related to the vertical pressure, the vertical pressures of the above three bearings in this study is taken as 25.5 kN to be consistent with the subsequent shaking table tests. The loading rate of the shear test is 0.01 Hz, using the displacement control, the tests for shear performance with the maximum shear displacement being 5 mm, 10 mm, 15 mm and 20 mm are carried out respectively, and each test is repeated by three times.

4.3 Analysis of the test results

Fig. 3 shows the shear hysteresis curve of three types of bearings respectively. As illustrated in Fig. 3(a), the sliding lead bearing achieved a well combination of the properties of both the lead bearing and frictional bearing. When the shear displacement of the bearing is small, the bearing mainly shows the sliding characteristics, which can meet the displacement demand of the bridge structure under the action of conventional temperature, vehicle braking force, concrete shrinkage and creep.

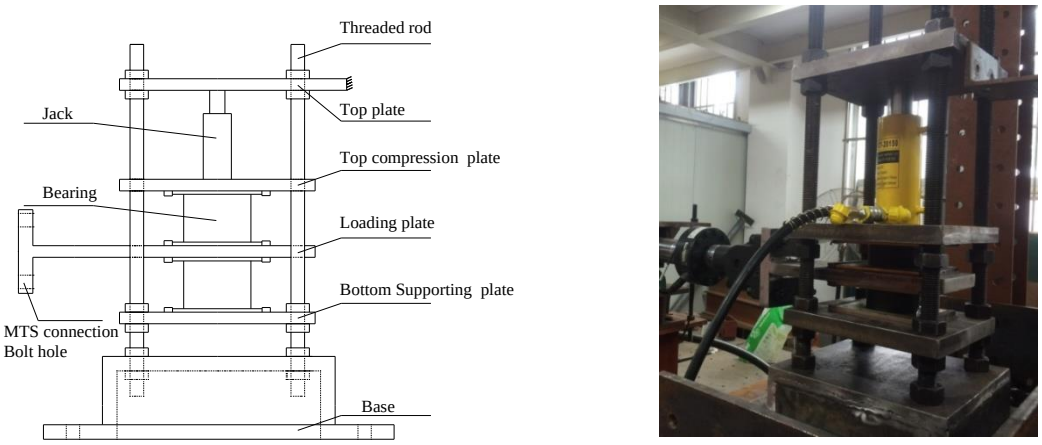

(a) Facade design (b) Molding diagram

Fig. 2 The loading equipment

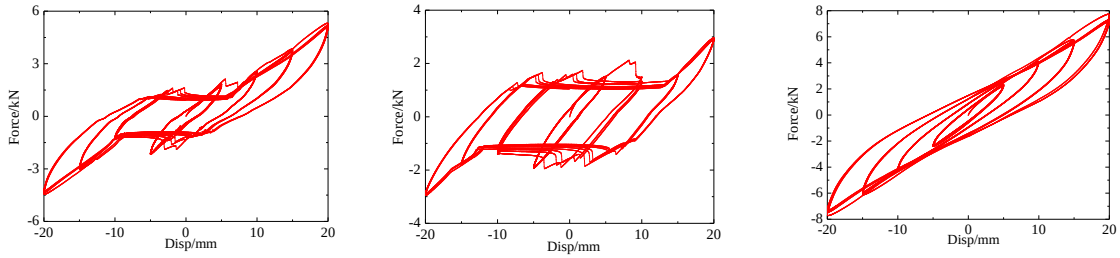

(a) Sliding lead rubber bearing (b) Sliding plate bearing (c) Lead-rubber bearing

Fig. 3 The hysteresis curve of the bearings

As the displacement increases and reaches the preset free-sliding threshold, the upper cover of the bearing contacts with the baffle, the bearing shows the energy dissipation characteristic and the horizontal force continues to increase at the same time. The stable sliding friction of the bearing is about 1.03 kN under the vertical pressure of 25.5 kN, in which the friction coefficient is assumed constant for simplicity (Wei *et al.* 2017), and it can be deduced that the sliding friction coefficient is about 0.044. It is worth noting that the maximum bearing shear force significantly exceeded the sliding friction force, but the bearing didn't slip when the maximum shear displacement of the bearing is 5 mm, which is mainly because the test loading rate is small and the maximum static friction of the bearing is greater than the sliding friction. it can also explain the phenomenon that the shear force of the bearing would be partially raised in each circle of the hysteresis curve when the bearing begins to slip. Fig. 3(b) shows the hysteresis curve of the sliding plate bearing, in which the sliding friction force is basically the same as that in Fig. 3(a). It should be pointed out that the area of the hysteresis loop is not 0 in the test with the maximum shear displacement being 5 mm, this phenomenon indicates that even using the natural rubber, it still acts some damping property. Fig. 3(c) is the hysteresis curve of lead rubber bearing, the hysteresis loop is full and the capacity of energy dissipation is strong, the maximum shear force of the bearing at the displacement of 20 mm reaches 8 kN.

From the first hysteresis loop shown in Fig. 3(b), the horizontal shear stiffness of the bearing under small shear deformation is about 0.338 kN/mm. From Fig. 3(c), it can be obtained that the yield strength of this lead core bearing is about 0.26 kN/mm.

According to the results in the previous section, the theoretical shear strength under small deformation of the plate bearing is 0.298 kN/mm, and the theoretical yield strength of the lead rubber bearing is 0.221 kN/mm. The errors of the two bearing between the theoretical and experimental results are lower than 15%, which may mainly result from the following three points: (1) The test can not exactly meet the boundary conditions required for theoretical solution, such as axial compression and bearings without any torsion. (2) The shear modulus of rubber is derived from Shore hardness by experience formula, and there exists some error itself. (3) The theoretical formulas of lead-rubber bearings are based on the results of a large number of bearings test, therefore, it is easy to understand that the test results obtained in this paper have certain errors with the theoretical results, especially considering that the bearings of this paper is of the small size and rarely used in normal projects. In general, the shear test equipment for small size bearings proposed in this paper has acceptable accuracy and practicability.

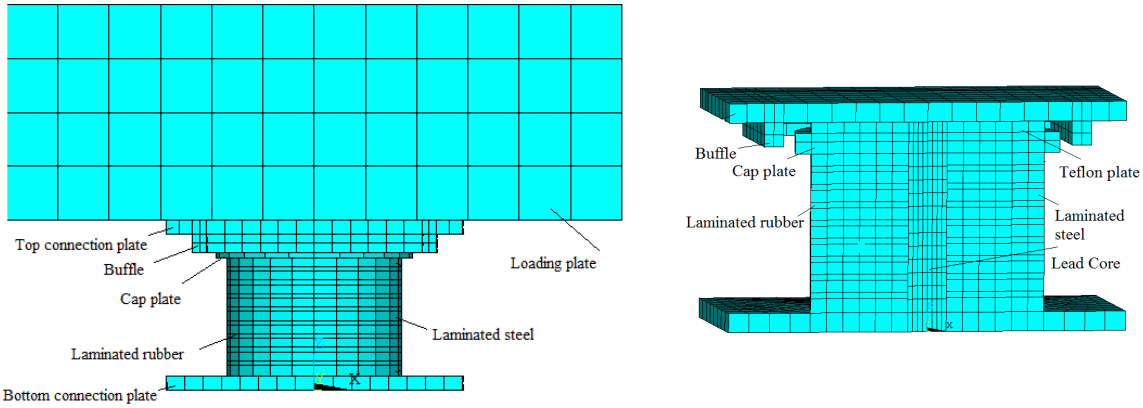

(a) Overall analytical model (b) Half-bearing cross section

Fig. 4 The FE model of the sliding lead rubber bearing

5. Numerical simulation

5.1 Finite element (FE) model of the bearings

In this paper, the ANSYS/LS-DYNA program is used to simulate the bearings mechanical properties based on explicit algorithm, the software is also used by Nie (2010) to simulate bearings. Taking the sliding lead rubber bearing as an example, the overall analytical FE model and the half-bearing cross section established in this study are shown in Fig. 4.

5.1.1 Basic settings and simplifications

(1) In order to control the computation cost, the reduced integration element is generally used in explicit dynamic analyses. However, this may cause the hourglass energy to be oversized, resulting in inaccurate or even incorrect results. This problem may be more serious in the case of unfair grid and excessive single-point concentrated force. In order to avoid this problem, the laminated steel plate, rubber layer and lead plug in this section are simulated by full integration elements, the rest use the reduced ones. Meanwhile, the hourglass energy controlling parameters are set reasonably.

(2) In the production of bearings, the laminated rubber and steel plate are vulcanized together and the other adjacent steel plates are connected by bolts, these relationships are simplified by common nodes in the FE model. In addition, the stainless steel plate is neglected in the model, that is to say, the top connection plate is in direct contact with the teflon plate.

5.1.2 Material parameter settings

As illustrated in Fig. 4, the laminated steel plate of the bearing is significantly thicker than the laminated rubber, which is obviously different from the design drawing shown in Fig. 2(a). The reason for making this adjustment is discussed in detail in another research (Wu *et al.* 2017), which can be summarized that the computation cost can be effectively reduced by enlarging the size of the laminated steel and the subsequent larger characteristic time step. In this section, the design parameters of laminated steels are modified and the mass scaling technology is utilized at the same time. The thickness of the steel plate is modified from the original 1.6 mm to 5 mm, the

elastic modulus is changed from 210 Gpa to 16.46 Gpa to be the same with the lead core, and the density is automatically adjusted by the program.

Except from the above parameters, other material parameters are set in accordance with the common used ones. The steel's Poisson's ratio is 0.3 and is characterized by elasto-plastic material with a yield strength being 235 MPa and a post yield stiffness ratio 0.1. The lead core is modeled by the ideal elastoplastic material, the yield strength is set as 9 Mpa, the Poisson's ratio is 0.44 and the elastic modulus is 16.46 Gpa. The Mooney-Rivlin model is used to characterize the super-elastic properties of the rubber material, the shear modulus, G, has the relationship of $G = 2(C_1 + C_2)$ with the two material constants of the model. According to the research results of Zheng *et al.* (2003), the material parameters, C_1 and C_2, are set as 0.36 Mpa and 0.04 Mpa. The elastic material is used to simulate the teflon plate, in which the modulus is determined as 300 Mpa, the Poisson's ratio is 0.4. The upper loading plate, which is different with that in Fig. 2, is mainly to simulate the actual loading conditions, the following vertical pressure and horizontal displacement is directly applied to the plate, so that they cannot affect the boundary condition of the bearing. The stiffness of the plate is much larger than the bearing, and the material parameters of the plate are the same with common steels.

5.1.3 Nonlinear contact relations

There exist many contact relations in the bearings described in this study, such as the sliding frictional contact between the teflon plate and the stainless steel plate, the contact between the lead plug and the surrounding rubber and steel plates, the possible contact between the baffle and the upper cap plate when large shear displacement of the bearing occurs, all these contact relationships can be simulated using the keyword of *CONTACT in ANSYS/LS-DYNA. Detailedly, the keyword of * CONTACT AUTOMATIC SURFACE TO SURFACE SMOOTH is used for the contact between the cap plate and the baffles, in which the coefficient of friction is set as 0.04; the keyword of * CONTACT ONE WAY AUTOMATIC SURFACE TO SURFACE SMOOTH is used for the sliding friction contact and the coefficient is 0.044. For the friction between the loading plate and the top connection plate, the first one is also utilized and the coefficient is 0.8 to ensure no slippage occurring between the loading plate and the top connection plate. The friction coefficient in all the above cases is set unchangeable in space and time for simplicity (Wei *et al.* 2018). The keyword *CONTACT TIED SURFACE TO SURFACE SMOOTH is employed to simulate the contact between the lead plug and the surrounding rubber and steels (Nie 2010, Wu *et al*. 2017).

5.2 Numerical simulation and result analysis

Based on the above finite element model, numerical compression-shear tests were carried out for three kinds of bearings in this section. For better simulating each test and considering the computation cost as well as the convergence issue, the boundary conditions of the FE model are set as follows: the displacement of the upper surface and the lateral surface of the loading plate along the x and y directions are both restrained and the pressure in the vertical direction (+z direction) is uniformly applied to each node at the top of the loading plate, the displacement of the bottom connection plate along the y and z directions is restrained, displacement along the x direction is applied to each node on the bottom plate of the bearing. All materials in the FE model do not consider the rate-dependent effect, that is to say, the loading rate has no effect on the numerical simulation results. In addition, the Bauschinger effect of the metal material and the

Payne effect of the rubber material are not taken into account in the numerical simulation. Considering that the loading rate of the previous experiment is rather small and each test is repeated by three times, the loading procedure is adjusted to one rather than three loading circles with the loading frequency 1 Hz in the numerical simulation. Theoretically speaking, the computation cost spent is 96.7% less than the non-adjustment.

5.2.1 Hysteresis curve

Fig. 5 shows the hysteresis curves of the bearing under compression-shear in accordance with the above numerical simulation, where the red line shows the experimental results in Fig. 3 and the black line shows the results of numerical simulation. The comparison indicates that the simulation results of the lead rubber bearing match the best with the test results, and there is a slight error for that of the sliding lead bearing, which mainly occurs in the small shear deformation. While the error between the two results of the sliding plate bearing is a bit larger. Main reasons for these differences are as follows: (1) the damping of the rubber material is not considered in the numerical simulation, the plate bearing loses its energy dissipation property after the sliding stage is finished, and the relation between the restoring force and shear displacement is approximately linear. While in experiment, the sliding bearing still behaves damping properties in this stage. (2) In the small deformation of the sliding lead bearing, the difference of pre-yield stiffness between numerical simulation and test is significant, which is mainly due to the ideal simplification of the lead material. (3) The difference between the dynamic friction coefficient and the static friction coefficient observed in the test results of the two sliding bearings is not considered in the numerical simulation. However, in general, numerical simulation of rubber bearings based on explicit numerical calculations described in this section is still fairly accurate and practicable.

5.2.2 Lead stress and strain state

Taking the sliding lead rubber bearing as example, Fig. 6 shows the stress-strain state of the lead at the maximum shear displacement of the bearing. As seen in Fig. 6(a), the length of the lead core is obviously elongated with a horizontal displacement of 5.23 mm at the top and 20 mm at the bottom, the displacement decreases approximately linearly along the height direction and meets the shear deformation characteristics. As can be seen from Fig. 6(b), the equivalent plastic strain of the lead core embedded in the bottom sealing plate of the bearing is 0. All other parts of the lead core is in the plastic stage, and the maximum equivalent plastic strain reaches 1.228, which means a large plastic flow deformation occurred.

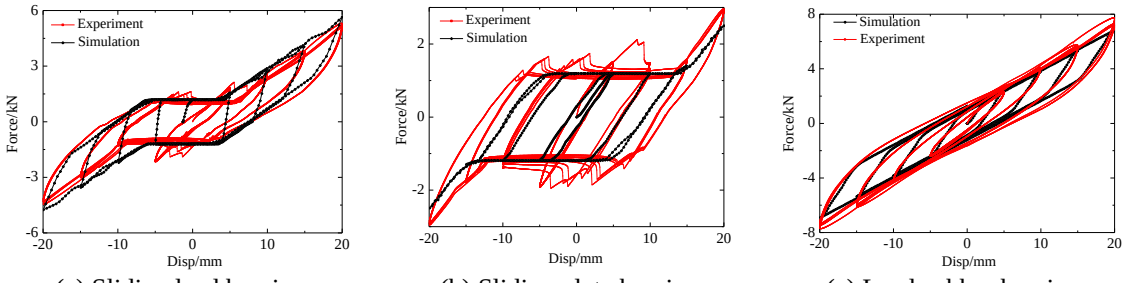

(a) Sliding lead bearing (b) Sliding plate bearing (c) Lead-rubber bearings

Fig. 5 The comparison of the hysteresis curves of bearings

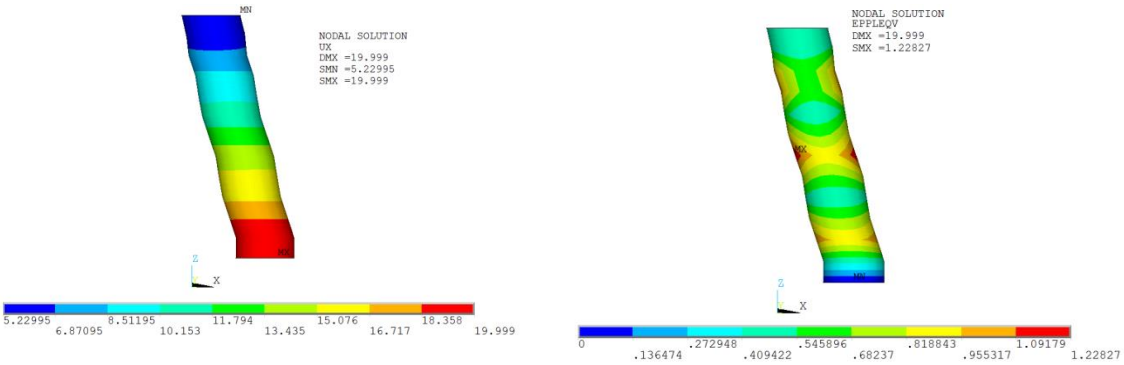

(a) Lead displacement (b) Equivalent plastic strain

Fig. 6 The state of the lead plug with the maximum shear displacement

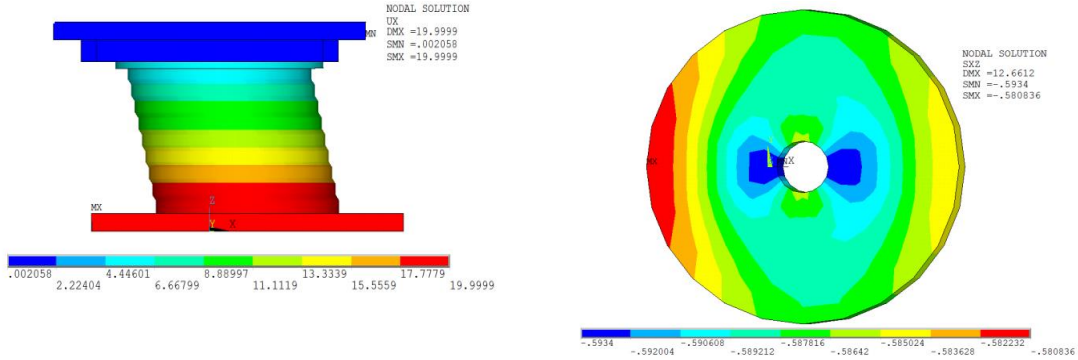

(a) Bearing displacement (b) Shear stress of the rubber plate

Fig. 7 The state of the rubber with the maximum shear displacement

5.2.3 Rubber stress and strain status

Fig. 7 shows the displacement contours of the bearing and the shear stress contours of the corresponding rubber plates at the maximum shear displacement of the sliding lead-rubber bearing. From Fig. 7(a) we can see the shear displacement of the bearing occurs mainly at the rubber plates of each layer, and the cap plate also touches the baffle with no gap existed. In Fig. 7(b), the maximum and minimum shear stresses of the rubber plates are 0.5934 Mpa and 0.5808 Mpa occurring at the center and edge of the rubber plate, which differ only about 2.1%. It is a good illustration that the shear stress of the rubber plate can be approximately assumed equal everywhere in the shear deformation. Furthermore, according to the design parameters of the bearing, it can be known that the shear displacement of 20 mm corresponds to 75% of the shear deformation of the rubber. Calculate by the simplified formula, $\tau = G\gamma$, the shear stress of the rubber plate is 0.6 Mpa, which shows a rather small error with the numerical result.

6. Conclusions

In this chapter, theoretical analysis, experimental research and numerical simulation of the compression-shear properties of the sliding lead rubber bearing, sliding plate bearing and lead-rubber bearing are carried out, the results are compared and verified, and some conclusions are drawn as follows,

- It can be seen from the test results that the sliding lead rubber bearing proposed in this paper can well obtain the combined properties of the lead rubber bearing and the sliding bearing.
- The equipment proposed and fabricated in this paper, which is specially applied to the compression-shear test of small-size bearings, is verified practicable.
- The explicit dynamic finite element analysis method based on ANSYS/LS-DYNA proposed in this paper can well realize the numerical simulation of the compression-shear test of three types of bearings. Analysis shows that the assumptions and simplifications of the analysis method make the computation cost significantly reduced, and the error is rather small.
- According to the comparison of the basic mechanical properties of the three bearings obtained from the theoretical analysis, experimental research and numerical simulation, it can be found that the method to study the basic mechanical properties of the bearing in this paper is verified accurate and practicable, which can be generalized for other types of bearings.

Acknowledgments

The authors would like to acknowledge the support from the National Natural Science Foundation of China (Grant No. 51578151), Beijing Advanced Innovation Center for Future Urban Design (No. UDC2016030200), the National Natural Science Foundation of China for Excellent Young Scholars (Grant No. 51722804) and the National Natural Science Foundation of China for Young Scholars (Grant No. 51508019).

References

Abe, M., Yoshida, J. and Fujino, Y. (2004), "Multi-axial behaviors of laminated rubber bearings and their modeling. I: Experimental study", *J. Struct. Eng.*, **130**(8), 1119-1132.

Ali, H-E. M. and Abdel-Ghaffar, A.M. (1995), "Modeling of rubber and lead passive-control bearings for seismic analysis", *J. Struct. Eng.*, **121**(7), 1134-1144.

Constantinou, M.C., Caccese, J. and Hawis, H.G. (1987), "Frictional characteristics of Teflon-steel interfaces under dynamic conditions", *Earthq. Eng. Struct. D.*, **15**(6), 751-759.

Han, X. and Warn, G.P. (2014), "Mechanistic model for simulating critical behavior in elastomeric bearings", *J. Struct. Eng.*, **141**(5), 04014140.

Haringx, J.A. (1950), *On highly compressible helical springs and rubber rods, and their application for vibration-free mountings*. Philips Research Laboratories, Eindhoven, Netherlands.

Hwang, J.S., Chiou, J.M. and Sheng, L.H. (1996), "A refined model for base-isolated bridges with bi-linear hysteretic bearing", *Earthq. Spectra*, **12**(2), 245-273.

Kelly, J.M. and Eidinger, J.M. (1978), *Experimental results of an earthquake isolation system using natural rubber bearings*, Reports No. UCB/EERC78/03, California, USA.

Liu, W.G. and Zhou, F.L. (1999), "Research on fundamental mechanic characteristics of lead rubber bearings", *Earthq. Eng. Eng. Vib.*, **19**(1), 93-99.

MCJ (Ministry of Construction of Japan) (1994), *Manual for Menshin design of highway bridges*. Earthquake Engineering Research Center, University of California, USA.

Mori, A., Moss, P.J., Cooke, N., *et al.* (1999), "The behavior of bearings used for seismic isolation under shear and axial load", *Earthq. Spectra*, **15**(2), 199-224.

Nie, S.F. (2010), "Research of mechanical properties and application of LRB in continuous beam bridge". Huazhong University of Science and Technology, Wuhan, China.

SAC (Standardization Administration of the People's Republic of China) (2006), *Rubber Bearings—Part II: Elastomeric Seismic-Protection Isolators for Bridges*, Standards Press of China, Beijing, China.

Takayama, M., Tada, H. and Tanaka, R. (1994), "Finite element analysis of laminated rubber bearings used in base-isolation system", *Rubber Chem. Technol.*, **65**(1), 46-62.

Tyler, R.G. and Robinson, W.H. (1984), "High-strain tests on lead-rubber bearings for earthquake loadings", *Bull. New Zealand National Soc. Earthq. Eng.*, **17**(2), 90-105.

Wang, R.Z., Chen, S.K., Liu, K.Y., *et al.* (2014), "Analytical simulations of the steel-laminated elastomeric bridge bearing", *J. Mech.*, **30**(4), 373-382.

Warn, G.P., Whittaker, A.S. and Constantinou, M.C. (2007), "Vertical stiffness of elastomeric and lead-rubber seismic isolation bearings", *J. Struct. Eng.*, **133**(9), 1227-1236.

Wei, B., Wang, P., He, X.H., *et al.* (2017), "Effects of friction variability on a rolling-damper-spring isolation system", *Earthq. Struct.*, **13**(6), 551-559.

Wei, B., Zuo, C.J., He, X.H., *et al.* (2018), "Numerical investigation on scaling a pure friction isolation system for civil structures in shaking table model tests", *Int. J. Nonlinear Mech.*, **98**, 1-12.

Wu, Y.F., Wang, H., Li, A.Q., *et al.* (2017), "Explicit finite element analysis and experimental verification of a sliding lead rubber bearing", *J. Zhejiang University-SCIENCE A*, **18**(5), 363-376.

Yoshida, J., Abe, M., Fujino, Y., *et al.* (2004), "Three-dimensional finite-element analysis of high damping rubber bearings", *J. Eng. Mech.*, **130**(5), 607-620.

Zhang, J.P., Zhou, F.L. and Liao S.J. (2001), "Shake table test study of bridge isolation system(I)-test significance and model design", *Earthq. Eng. Eng. Vib.*, **4**, 128-134.

Zheng, M.J., Wang, W.J., Chen, Z.N., *et al.* (2003), "Determination for mechanical constants of rubber Mooney-Rivlin model", *Rubber Ind.*, **50**(8), 462-465.